Nonradiative Energy Transfer in Li*(3p)−CH_4 Collisions

Solomon Bililign*,† and Brian C. Hattaway

Department of Physics, North Carolina A&T State University, Greensboro, North Carolina 27411

Gwang-Hi Jeung*,‡

Laboratoire Aimé Cotton (Bât. 505) and ASCI (Bât. 506), Campus d'Orsay, 91405 Orsay, France

Received: July 10, 2001; In Final Form: October 4, 2001

The direct collisional energy transfer process Li*(3p) + CH_4 → Li*(3s) + CH_4 is investigated both theoretically and experimentally. We measured the nonreactive far-wing absorption profiles of the LiCH_4 complexes by monitoring the Li(3s) → Li(2p) fluorescence at 812.6 nm. The intensity of the Li(3s) → Li(2p) fluorescence decreases with detuning, indicating a more efficient transition rate at low detuning. A high level ab initio calculation in both C_{2v} and C_{3v} symmetry is performed to provide a general picture of the nonradiative transition induced by collisions between lithium atoms and a methane molecule.

I. Introduction

The interaction of hydrocarbon molecules with metal sites is of fundamental and practical interest. The activation of the C−H bond by metal atoms has attracted much attention.[1] Bulk phenomena like physisorption, chemisorption, and many homogeneous and heterogeneous catalytic processes might be better understood if we knew details of the chemical and physical binding of hydrocarbon molecules with metal atoms. Even though some work has been done with quenching of alkaline earth metals [2−5] by methane, which is the simplest hydrocarbon, there is very little or no work done on quenching of alkali atoms by methane or any other hydrocarbon.[6−8] Despite the fact that the C−H bond in methane is weaker than the H−H bond of H_2 while excited K atoms were found to react with H_2 to yield KH, no KH product was detected when H_2 was replaced by CH_4.[9] It is argued that the large size of the K atom might cause steric effects, making the K−CH_4 insertion reaction unfavorable. The situation is quite different with group II metals. For example,[4] Mg(3s3p $^1P_1$) and Zn(4s4p $^1P_1$) atoms react with both CH_4 and H_2 to yield MgH or ZnH. While the M(nsnp, $^3P_1$; M = Mg, Zn, Cd, Hg) states are highly reactive with the H−H bond, they react inefficiently with the C−H bond. It is believed that the reason the M($^1P_1$) singlet states react with alkanes with no activation barriers while the triplet M($^3P_1$) states cannot is that there is a better energy match and thus better overlap between the M(np) orbitals of the singlet states with the localized C−H(σ*) orbitals than for the triplet states. The C−H(σ*)−M(np) interaction would be thus sufficiently strong to override the electron−electron repulsion from neighboring C−H or C−C bonds or from C−H(σ)−M(ns) overlap.

The far-wing scattering technique has been applied recently to study the interaction between the metal atom and the methane molecule. Kleiber and co-workers[10,11] studied the effect of electronic orbital alignments in the reaction of Mg*(3s3p $^1P_1$) + CH_4 → MgH + CH_3 and proposed that the reaction proceeds in η_2 geometry through a triangular C−Mg−H transition state.

Lithium is useful as a synthetic reagent in organic and organometallic chemistry, and the nature of the lithium−carbon bond may be of interest.[12] To the best of our knowledge the only work on the quenching of Li by CH_4 were the theoretical studies by McCaffrey and co-workers[13] and Chaquin and co workers.[14] Chaquin[14] performed a theoretical study of the quenching of the low-lying excited states of Li by CH_4. He observed no energy barrier above endothermicity for the CH_4 + Li → CH_3 + LiH reactions for both insertion and abstraction model mechanisms. He found that the potential energy surfaces (PES's) originating from the lowest excited Li(2p ^2P) state of Li are strongly repulsive and he ruled out both reactive diabatic and adiabatic processes. A bound state was observed for higher energy states, Li(3s^2 S) and Li(3p^2 P). They argued qualitatively that the compact valence states of Li(1s^2 S) and Li(2p^2 P) experience the electronic repulsion of the C−H bonds without sufficient overlap of metal AO's with σ* MO's of CH_4 leading to repulsion, while for the more diffuse orbitals, as in Li(3s^2 S) and Li(3p^2 P), the overlap is greater. On the basis of this they predicted the possible formation of vibrationally excited LiH with a small rotational excitation energy.

In this work, we report an experimental and theoretical study of the nonradiative energy transfer in Li(3p)−CH_4 collisions. We used the far-wing scattering technique to investigate the quenching of Li(3p^2 P) by CH_4. We looked at two possible nonreactive processes from the Li(3p) initial state:

$$\mathrm{Li(2s) + CH_4} + h\nu \rightleftharpoons [\mathrm{Li(3p)CH_4}]^* \rightleftharpoons \mathrm{Li(3p) + CH_4} \quad (1a)$$

$$\rightleftharpoons \mathrm{Li(3s) + CH_4} \quad (1b)$$

The far-wing scattering technique explained in detail in previous works[15,16] offers a direct probe of the continuum or "scattering states" of a transient bimolecular collision complex. This technique can be used to selectively excite quasimolecular electronic states of well-defined symmetry corresponding to a specific electronic orbital alignment of the reagents within the transient reaction complex. The spectra reflect the shape of excited-state potential energy surfaces. Final state resolved measurement of the far-wing fluorescence spectrum depends

* To whom correspondence should be addressed.
† E-mail: Bililign@ncat.edu. Fax: (336) 256-0815.
‡ E-Mail: Jeung@asci.fr.

10.1021/jp012616w CCC: $22.00
Published on Web 12/14/2001

on the dynamical evolution of the system in the excited state, and it provides an insight into the effects of electronic orbital alignment, nuclear motion dynamics and nonadiabatic effects in this evolution.

To understand the experimental results, we also have performed a high level ab initio calculation. A large flexible basis set has been used together with a large-scale configuration interaction to obtain reliable potential energy surfaces involved in the title reaction. The quasistatic line shape theory based on the calculated ab initio results is used to understand some of the observed features in the far-wing absorption profile.

II. Experimental Details

The experimental setup is similar to the one described in previous works.[16,17] Briefly, the doubled and tripled frequencies of a 20 Hz Nd:YAG laser were used to pump two dye lasers simultaneously in a laser pump−probe arrangement. The pump dye laser used here was operated using a DCM dye whose output is frequency-doubled to the spectral region of the Li(2s−3p) second resonance transition at 323.3 nm. The pump laser pulse had a typical pulse width of 4−6 ns and pulse energy of 200 μJ. The five-arm stainless steel heat pipe oven contains Li vapor and the quenching gas (CH_4) and is resistively heated to a temperature of 900 K. This corresponds to a Li atom vapor density of $\sim 10^{13}/cm^3$. The typical operating pressure of the buffer gas (CH_4) was 6−8 Torr, and the pressure was measured with a capacitance manometer.

The nonreactive profile is determined indirectly by monitoring the cascade fluorescence on the Li(3s−2p) atomic transition at 812.6 nm. The direct atomic fluorescence from the laser excited Li($3p^2$ P) state to the ground state is very weak due to heavy radiation trapping, and it was difficult to resolve the atomic fluorescence from the scattered near-resonant pump laser light and detect the population of the 3p state directly. We therefore chose to do the measurement indirectly. We measured the direct collisional quenching of the Li(3p)CH_4 complex to the Li(3s) state by monitoring the cascade fluorescence of the Li(3s−2p) atomic transition at 812.6 nm. The temporally integrated signal intensity is then measured as a function of detuning of the laser in the red and blue wings of the Li(2s −3p) transition. It is worth noting that the Li(3s) state may be populated by either fluorescence from the Li(3p) state or by direct collisional quenching of the $LiCH_4$ state to the 3s state. Experimentally we do not distinguish between these possible pathways for producing the Li(3s) state. However, as indicated below, we believe that the radiative excitation pathway can be neglected relative to the collisional pathway.

The fluorescence is collected using a lens and a steering mirror assembly by a 35 cm McPherson monochromator with 1200 lines/mm holographic grating. The fluorescence is detected with a photomultiplier, and the signal output is amplified using a fast preamplifier and analyzed using a gated integrator/boxcar averager system. The output was averaged over 300 pulses. The pump laser intensity is monitored with an energy meter and the far wing profiles were normalized to constant incident energy.

Nonlinear processes in general may lead to strong photoionization, self-focusing, parametric amplification, and stimulated atomic emission processes. These problems are more significant near the line center (resonance) and at high pump laser power. We have verified that the Li* signals are linear in the pump laser beam intensity, by measuring the fluorescence as a function of pump laser power at different detuning, both near the line center and in the wings. We also measured the fluorescence signals as a function of CH_4 pressure in the range 2−10 Torr, and they were linear, indicating that secondary collisions could be ruled out under the conditions of our experiment.

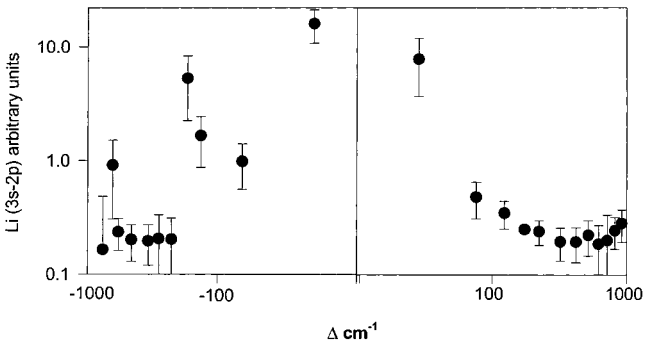

Figure 1. log−log plot of the experimental far red-wing and blue-wing absorption profiles for the ($LiCH_4$) complex. Nonreactive Li(3s−2p) fluorescence signal as a function of pump laser detuning ($\Delta = \omega_L - \omega_o$) from Li(2s−3p) atomic resonance transition.

III. Experimental Results

The main experimental results of this work are presented in Figure 1. It shows the relative population in the nonreactive product channel corresponding to the process (1b) in the red and blue wings. We assume the 3p−2s radiative decay rate is small enough that spontaneous emission can be neglected relative to the collisional relaxation process. Furthermore, as indicated in the Experimental Section, the effect of stimulated atomic processes can be neglected under our experimental conditions. At higher laser power or temperature, stimulated emission from Li(3p) was clearly present and resulted in a very strong fluorescence, signals with rapid rise and fall times, which was independent of gas pressure. We have also verified that this effect was strong near the line center, i.e., resonance. We therefore assumed under the conditions of our experiment, that the direct fluorescence from the Li(3p) is negligible, and we further assumed that direct collisional energy transfer is more important and consistent with the process wherein the complex $LiCH_4$ predissociates rapidly to Li(3s) followed by fluorescence of Li(3s).

It is also worth noting that the 3s−2p fluorescence signal is significantly more intense than a similar signal with H_2 as a quenching gas, the experimental conditions being about the same in the two cases. This may indicate several possibilities. Either the quenching cross section is much larger for Li−CH_4 than for Li−H_2 or the overall far wing absorption cross section might be larger for Li−CH_4 than for Li−H_2 or the radiating states might be more efficiently quenched by H_2 than by CH_4, leading to a lower radiative yield in the H_2 case.

Even though the possibility of forming stable Li(3p)CH_4 complexes and possible formation of vibrationally excited LiH with low rotational energy is predicted in the theory, in our present work we were not able to detect any LiH in the $v'' = 1$ state. This does not rule out the possibility of detecting LiH in the ground vibrational state or low rotational states of the vibrationally excited LiH states. However, our current experimental setup did not allow us to investigate this possibility further. Our search for reactive products will continue in future works, and in this paper we will concentrate on the nonreactive absorption of the complex.

IV. Computational Method

We have used a large atomic basis for the lithium atom to represent the 2s, 2p, 3s, 3p, and 3d states. For this, the

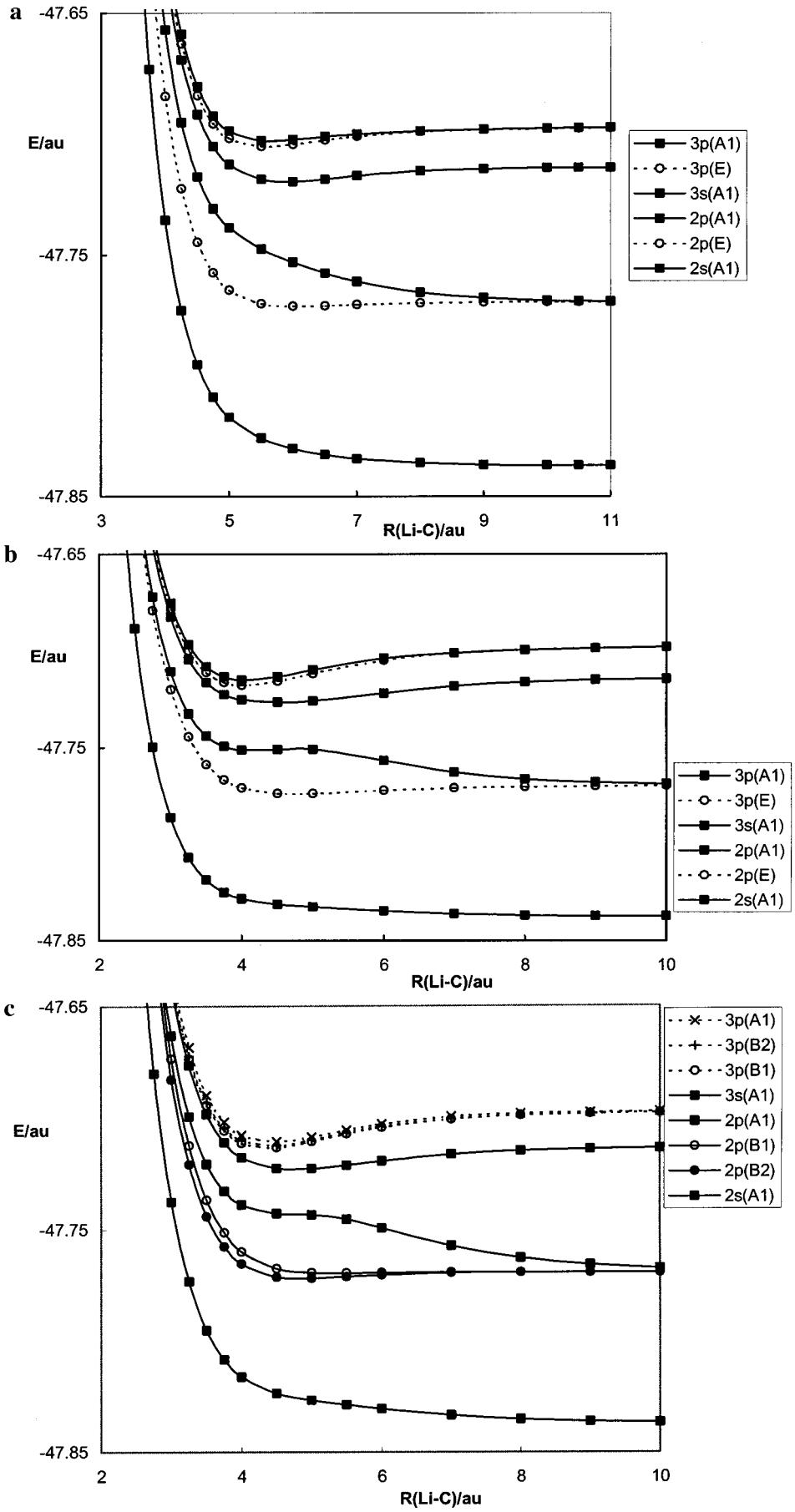

Figure 2. Three sections of the potential energy surfaces for $Li-CH_4$ (R and E in au): (a) a single hydrogen atom lying between the lithium atom and carbon atom of methane in C_{3v} (η_1); (b) three hydrogen atoms atom lying between the lithium atom and carbon atom of methane in C_{3v} (η_3); (c) two hydrogen atoms atom lying between the lithium atom and carbon atom of methane in C_{2v} (η_2).

15s10p6d3f Gaussian type orbitals (GTOs) were used without contraction. The 13s8p2d GTOs were used without contraction for the carbon atom and the 7s3p GTOs were used without contraction for the hydrogen atoms. The C−H distance of the methane molecule has been fixed to 2.08 bohr, which is close to the experimental value. The method of computation used in this work is similar to a work on Li−H_2.[18] The molecular orbitals were obtained from the state-averaged complete-active-space (CAS) self-consistent-field calculations using the 13 active orbitals originating from Li(2s) to Li(3d) atomic orbitals. Then multireference (MR) configuration interaction (CI) calculations were done. In this case, the valence electron coming from Li was distributed to the active molecular orbitals according to the state symmetry. Then, all possible single and double excitations of the nine valence electrons were used to generate the configuration state functions. This includes a limited number of triple excitations. The final energies were obtained by diagonalization of the CI matrix.

Three geometrical forms were studied here. The notation η_n will be used to designate the specific geometry. In this notation n is the number of H atoms that face the Li atom. The first geometry is of C_{3v} symmetry with the Li−C−H atoms forming a straight line where Li faces three hydrogen atoms (denoted as η_3 or C_{3v}/3H). The second is also of C_{3v} symmetry with the Li−H−C atoms forming a straight line where Li directly collides with one hydrogen atom (denoted as η_1 or C_{3v}/1H). The third is of C_{2v} symmetry where Li faces two hydrogen atoms (denoted as η_2 or C_{2v}/2H). For the C_{3v} symmetry cases, we have used a lower symmetry, the C_s symmetry, in our calculations. In this case, the A′ symmetry states include the A_1 and E states. We could not include the core-valence correlation effect for the Li core in this work because of the too large CI matrix. Indeed, for the A′ representation, the total number of configurations generated in valence-only CI calculations that we performed is already 934 702. The inclusion of the core single excitation to the valence-only CI was not practical. This is the main difference with the previous work on Li−H_2.[18] We did not attempt to vary the C−H distances in this work as the number of geometries to calculate is beyond the practical limit.

The atomic asymptote Li(2s), Li(2p), Li(3s), Li(3p), and Li(3d) states are separated by 14 851, 12 038, 3739, and 267 cm^{-1} in our calculation, which should be compared to the experimental atomic excitation energies 14 904, 12 302, 3719, and 358 cm^{-1}, respectively.[19] The underestimation of the atomic excitation energy, which is the largest in 3s−2p, is due to the omission of the core-valence correlation effect of the lithium atom. This omission also leads to a too small 3d−3p energy difference in comparison to the experimental data.

V. Theoretical Results

The three sections of the potential energy surfaces corresponding to the above-mentioned geometrical forms are shown in Figure 2. The Li(2s)−CH_4 is repulsive and cannot make a stable complex. The Li(2p)−CH_4 forms one (C_{2v}) or two degenerate (C_{3v}) weakly attractive states and a repulsive state. However, the repulsive 2p state forms a shallow potential well due to an avoided crossing with the attractive 3s configuration, as can be seen in Figure 2b. The Li(3s)−CH_4 and Li(3p)−CH_4 form stable complexes. Four of the five Li(3d)−CH_4 states are attractive and one A_1 state is repulsive. The repulsive or attractive nature of each electronic state follows the general rule concerning the interaction between one metal atom and a compact structure like a rare-gas atom.[20] The Li−C bond distances and the binding energies for the excited complexes are shown in Table 1.

TABLE 1: Li−C Distance and Bond Energy of the Li−CH_4 Excited Complexes in C_{3v}/1H (η_1) Geometry

state	symmetry	R(Li−C), pm	bond energy, cm^{-1}
3d	A_1	215	3970
3p	E	214	4480
3s	A_1	235	2680
2p	E	248	1020

The diabatic coupling between Li(2p) and Li(3s) is strong and leads to a widely avoided crossing between the 2^2A_1 and 3^2A_1 states in the three geometric forms we studied. This is different from the Li−H_2 case where a repulsive state of Li(2p)−H_2 makes a closely avoided crossing with the Li(3s)−H_2 state.[16,17] The electronic states originating from the 2s, 2p, and 3s atomic asymptotes are well separated from each other. The three electronic states originating from the 3p atomic asymptote are weakly split even for short Li−C distances. This means that the 3p atomic orbital is so diffuse that the interaction with the electrons of methane does not depend on the orientation of the atomic orbital. The wave functions for all these states show significant mixtures of different angular momentum functions.

In compact geometry, i.e., for a short Li−C distances, the energy difference between the Li(3s)−CH_4 and Li(3p)−CH_4 states is small. We show a close-up view for the potential curves for the 3s and 3p states together with the lowest 3d state ($5\ ^2A_1$) in Figure 3. In this figure, the dissociation limits of Li(3s), Li(3p), and Li(3d) are translated to agree to the experimental data. This decreases the Li(3p−3s) difference by 8 cm^{-1} and increases the Li(3d−3p) difference by 91 cm^{-1}. This adjustment is relatively minor in comparison with the potential energy variations of the molecular states as can be seen in Figures 2 and 3.

VI. Discussion

The general shape of the potential energy surfaces looks much similar to the potential curves of the lithium/rare-gas cases. However, the nonspherical symmetry of the methane molecule differentiates quantitatively the potential energy surfaces in the three symmetries studied in this work.

We first consider seeing if there exists a one-to-one correspondence between the detuning and the molecular geometry in far-wing excitation. In far-wing studies of the diatomic system, it is generally agreed that there exists a simple relationship between the laser detuning and the internuclear distance, R_o (Condon point), where excitation occurs. For polyatomic systems, there is no such one-to-one correspondence when we take all possible degrees of freedom. However, a weak analogy can be established if we consider only the intermolecular degree of freedom, e.g., the Li−C distance. In general, small detuning corresponds to an excitation of the ground-state molecule at large Li−CH_4 distances and large detuning corresponds to a shorter distance. Nevertheless, the shortest possible Li−CH_4 distance is solely determined by the repulsiveness of the ground-state potential surface and the maximum relative kinetic energy that most of the reactants can attain. For formation of the Li(2s)−CH_4 molecule at 5 bohr, for example, the reactant should have at least 0.54, 0.28, and 0.12 eV for the C_{3v}/3H, C_{2v}/2H, and C_{3v}/1H geometries, respectively. It means that the really short distances are never attained for the initial ground state. Only after the pumping excitation can the excited-state evolve to the short distances through the internal vibration. In fact, for the detuning range we have used in this work, about 900 cm^{-1}, only the long distance part of the ground state is excited. This can be easily checked by comparing the binding

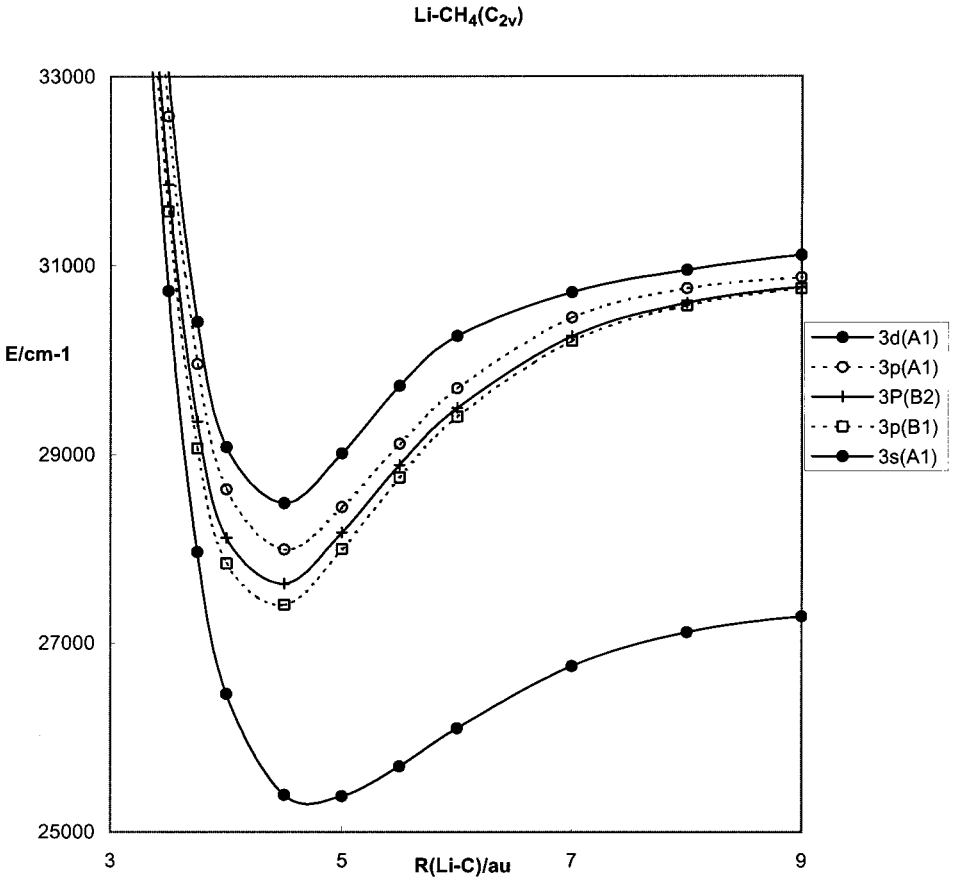

Figure 3. Enlarged C_{2v} section for the 3s, 3p and 3d(A_1) states of Li−CH_4 (R in a.u. and E in cm^{-1} with respect to the Li(2s) + CH_4).

energies of the excited complexes in Table 1 to the detuning energy, remembering that the energy difference between the ground and the excited states corresponds to the pump laser energy.

The quenching of the Li(3p) to the Li(3s) state indicated in Figure 1 can be easily understood from the close approach between the 3s and 3p potential energy surfaces in Figure 3. The attractive potential of the Li(3p)−CH_4 state should lead to a close contact between the lithium atom and the methane molecule in all collision geometries. As the thermal energy in our experimental condition is much larger than the energy difference between these two potential energy surfaces at short Li−C distances, the 3p to 3s transition should be easy. In this kind of nonradiative transition, two factors are important to determine the transition probability. One factor is the energy difference as a function of the distance and the diabatic coupling as appears in the Landau−Zener−Stückelberg model. The smaller the energy difference, the easier it is for nonradiative transition. The larger the diabatic coupling, the easier it is for nonradiative transition. We could not evaluate the diabatic coupling function (i.e., coupling of the nuclear Hamiltonian to the electronic wave function), as there is no general method to evaluate this term for polyatomic systems. However, the significant intermixture of the s and p type basis functions in the Li(3p)−CH_4 and Li(3s)−CH_4 states indicate that the diabatic coupling may be significantly large.

Another determining factor for the nonradiative transition probability is the number of collisions between Li and CH_4. Indeed, the total transition probability is directly proportional to the number of collisions during the lifetime of each electronic state. Here, one might note that the Li(3p)−CH_4 and Li(3s)−CH_4 states are all dynamically bound. Those states have a stable potential well below the asymptotic energy level corresponding to the $LiCH_4$ complex. On the other hand, even for the energy level somewhat higher than the asymptotic level, where the initial collision begins, the potential surface is repulsive only for one degree of freedom, R(Li−C). Varying the coordinate along other internal vibrational modes leads to a potential wall. Schematically, one can imagine a very narrow valley leading to a basin surrounded by a high cliff. It is easier to enter than to get out. This is the situation, which we call the dynamically bound case.

The red-shift absorption wing corresponds to the excitation to the potential well below the asymptotic limit of Li(3p). It is true that free-free excitation dominates at small detunings; however, free-bound absorption dominates as detuning increases. Here, the lifetime is determined by the radiative lifetime and is usually much longer than the duration of a single collision or vibration. The Li(3p)−CH_4 complex would pass a long time with a large number of internal vibrations. Once the electronic transition occurs at a long distance (R_+) corresponding to the red shift, the attractive potential of the 3p excited states allows a close contact between the metal atom and the methane molecule up to the short distance (R_-) having the same energy level as the reactant energy. It is around R_- that the nonradiative transition occurs, as the 3p and 3s potential energies are close. The minimum energy difference between the 3p and 3s lies around 3.6 bohr with the potential energy far larger than the 3p asymptote. As a consequence, the nonradiative transition should decrease as the negative (lower-frequency) detuning increases. So, one might expect a more efficient transition rate for small detuning and then a general decrease of the transition as the detuning increases. Figure 1 seems to follow such pattern. A better account of the transition rate should take into account the internal vibrational states of Li(3p)−CH_4 and the integrated transition rate over the vibrational degrees of freedom, which

could result in the transition rate deviating from the simple picture. There is indeed a singular increased transition rate visible in a far red-shift region. We did not attempt this kind of fine analysis in this work.

The blue-shift absorption corresponds to the excitation to the dynamically bound (small shift) and repulsive part (large shift) of the potential surface. Figure 3 shows that the energy difference between the Li(3p)−CH_4 and Li(3s)−CH_4 states becomes smaller at higher energies in the inner wall. This alone should favor a more efficient transition between 3p and 3s states for a larger detuning. However, the dynamical stability decreases for the increasing detuning to become purely repulsive, in which case only a single collision involving two surface hoppings would happen. Thus a further increase in the collision energy would rapidly decrease the lifetime. The combination of these two factors is expected to lead to a large transition rate near the line center and then to a decreasing rate as detuning increases. However, the data also show a slight increase in the far-blue wing, as shown in Figure 1. We cannot explain the slight increasing tendency seen at the extreme far-wing.

There is another factor to consider in the blue-shifted electronic transition. That is the intermixture of the atomic configurations in the molecular states. Indeed, the s-, p-, and d-like atomic configurations lose their purity as soon as the perturbing molecule approaches to the metal atom, in particular for the Rydberg states where the electron distribution is very diffuse. This may bring about transitions between 3d−2s or 3s−2s states, which are dipole forbidden at long intermolecular distances.

Assuming CH_4 as a spherical purturber, and making comparison to the Li−Kr system, we can also get some insight and rationalize the experimental far-wing absorption profile leading to nonradiative quenching by using a simple quasistatic line shape analysis. Considering the complexity of the system, this approach may be an oversimplification. However, we can extract some general features. We fitted the calculated potentials to a simple Buckingham type potential to extract the C_6 coefficient for the ground and excited states for all geometries calculated, η_1, η_2, and η_3. We also used the experimental and calculated values of C_6 for Li−Kr as a fixed parameter in the fitting. For Li−Kr a range of values is given in the literature, ranging from an experimental value of −280 au [21] and two theoretical values of −250[22] and −389 au.[23] In our fitting procedure, the value −389 au overestimates the Li−CH_4 potential well depth. The value we obtained from the best fit to the ab initio potential curves was 300 au. Using these C_6 coefficients, we estimated the distance R_o (Condon point) for the range of detuning used in this experiment; 20−500 cm^{-1} in the red wing and 20−900 cm^{-1} in the blue wing. The range of Li−C distance is estimated to be 6.8 au (3.6 Å) < R_o < 12.5 au (6.2 Å) in the red wing and 6.23 au (3.3 Å) < R_o < 12.5 au (6.2 Å) in the blue wing.

It is known from atom−atom collisional broadening studies within the quasistatic approximation, the absorption profiles are sensitive to the shape of the difference potential. For all the calculated potential symmetries the difference potential decreases monotonically, except for a very small barrier in the E state (η_3), all the way to very small internuclear distance, and a minimum appears at a very short internuclear distance R < 4.5 au (2.4 Å), which is far beyond the range of detuning in this experiment.

The large number of degrees of freedom did not allow us to go further in theoretical study beyond the three symmetrical cases. However, we believe that the general picture of the nonradiative transition induced by the collision between a lithium atom and a methane molecule could be deduced from this work. A detailed work that provides information on the nonadiabatic coupling between the potential surfaces in the Li−CH_4 system is beyond the scope of the current work. We hope this initial study will stimulate further work in this direction.

Acknowledgment. S.B. and B.C.H gratefully acknowledge the financial support of the National Science Foundation (CHE-9733744). The CNRS also partially supported this work.

References and Notes

(1) Steacie, E. W. R *Atomic and Free Radical Reactions*, 2nd ed.; Van Nostrand Reinhold: New York, 1954; Vols. I and II.
(2) Breckenrgide, W. H.; Umemoto, H. The Dynamics of the Excited State. In *Advances in Chemical Physics*; Lawley, K., Ed.; Wiley: New York, 1982; Vol. 50.
(3) Breckenrgide, W. H. In *Reactions of Small Transient Species*; Clyne, M., Fontijin, A., Eds.; Academic: London, 1983.
(4) Breckenrgide, W. H. *J. Chem. Phys.* **1996**, *100*, 14840 and references therein.
(5) Breckenrgide, W. H.; Umemoto, H. *J. Chem. Phys.* **1981**, *75*, 698; **1982**, *77*, 4464; **1984,** *81*, 3852.
(6) Earl, B. L.; Herm, R. R.; Lin, S.-M.; Mims, C. A. *J. Chem. Phys.* **1972**, *56*, 867.
(7) Earl, B. L.; Herm, R. R. *J. Chem. Phys*. **1974**, *60*, 4568.
(8) Gallagher, T. F.; Ruff, G. A.; Safinya, K. A. *Phys. Rev*. **1980**, *A22*, 843.
(9) Ke, C. B.; Chou, S. H.; Lin, K. C. *J. Chem. Phys*. **1993**, *93*, 604.
(10) Wong, T. H.; Kleiber, P. D. *J. Chem. Phys* **1995**, *102*, 6476.
(11) Wong, T. H.; Freel, C.; Kleiber, P. D. *J. Chem. Phys*. **1998,** *108*, 5723.
(12) Streitwieser, A.; Williams, J. E.; Alexandrato, S.; McKelvey, J. M. *J. Am. Chem. Soc.* **1980**, *102*, 4572. Graham, G. D.; Marynick, D. S.; Limpcomb, J. D. *J. Am. Chem. Soc*. **1980**, *102*, 4572.
(13) McCaffrey, J. G.; Poirier, R. A.; Ozin, G. A.; Csizmadia, I. G. *J. Phys. Chem*. **1984**, *88*, 2898.
(14) Chaquin, P.; Papakondylis, A.; Giessner-Prettre, C.; Savin, A. *J. Phys. Chem.* **1990**, *94*, 7352.
(15) Kleiber, P. D. In *Chemical Dynamics and Kinetics of Small Radicals*; Liu, K., Wagner, A., Eds.; World Scientific: Singapore, 1996. Kleiber, P. D.; Stwalley, W. C.; Sando, K. M. *Annu. Rev. Phys. Chem*. **1993**, *44*, 13.
(16) Bililign, S.; Kleiber, P. D.; Kearney, W. R.; Sando, K. M. *J. Chem. Phys*. **1992**, *96*, 218.
(17) Bililign, S.; Hattaway, C. B.; Geum, N.; Jeung, G.-H. *J. Phys. Chem. A* **2000**, *104*, 9454.
(18) Lee, H. S.; Lee, Y. S.; Jeung, G.-H. *J. Phys. Chem*. *A* **1999**, *103*, 11080.
(19) Moore, C. E. *Atomic Energy Levels*; Natl. Bur. Stand. (US) Cir. No. 467; U.S. GPO: Washington, DC, 1971; Vol. 1.
(20) Yiannopoulou, Y.; Jeung, G.-H.; Park, S. J.; Lee, H. S.; Lee, Y. S. *Phys. Rev*. **1999**, *A59*, 1178.
(21) Rothe, E. W.; Neynaber, R. H. J. *Chem. Phys*. **1965**, *42*, 3306.
(22) Dalgarno, A.; Davidson, W. D. *Adv. At. Mol. Phys*. **1966**, *2*, 1.
(23) Mahapatra, P. C.; Rao, B. K. *Int. J. Pure. Appl. Phys*. **1987**, *25*, 331.